A Parabolic Torus Compact Antenna Test Range for 5G NR Massive MIMO OTA Multi-User Test Applications

S.F. Gregson[1, 2]
[1] Next Phase Measurements
11521 Monarch St, Garden Grove, CA, USA
stuart.gregson@qmul.ac.uk

C.G. Parini[2]
[2] Queen Mary University of London
10 Godward Square, London, UK
c.g.parini@qmul.ac.uk

***Abstract*— This paper presents a novel design for a compact antenna test range (CATR) that uses a parabolic toroid as the main reflector which possesses superior pseudo-plane wave scanning capabilities than existing comparable CATR designs. The wide-angle scanning capability is a crucial feature for successful over-the-air test and measurement of mm-wave 5G NR Massive Multiple Input Multiple Output (MIMO) antenna systems in multi-user applications where existing far-field multi-probe anechoic chamber (FF-MPAC) systems become unattractive due to their large far-field distance requirements. CATR quiet-zone results are presented and discussed.**

Keywords—Parabolic-Torus CATR, Far-Field Multi-Probe Anechoic Chamber, FF-MPAC, 5G NR, Massive-MIMO, OTA

I. Introduction

Direct far-field (DFF) testing has become the de facto standard for sub-six GHz over the air (OTA) testing of the physical layer of radio access networks [1, 2] with the far-field multi-probe anechoic chamber (FF-MPAC) becoming especially widely deployed for the verification of massive multiple input multiple output (MIMO) antennas in the presence of multiple users [1, 2]. The adoption of mm-wave bands within the 5th generation new radio (5G NR) specification has meant that, as these systems require the user equipment be placed in the far-field of the electrically large base transceiver station (BTS), either excessively large FF-MPAC test systems are required, or the user equipment is placed within the quiet-zone of a compact antenna test range (CATR) [3]. Standard CATR based methods do not permit far-field OTA testing of Massive MIMO antennas in multiple user scenarios as the CATR is only capable of producing a single pseudo plane. However, it is possible to steer the direction of the pseudo plane wave by displacing the CATR feed from the focal point [4]. Beam steering such as this is sought at the price of increasing the phase taper within the CATR quiet-zone (QZ) however that can be partially mitigated by translating the feed towards the reflector with an acceptable compromise between CATR QZ amplitude taper & ripple, and phase taper being generally achievable for pseudo plane wave scan angles of up to *circa* ±15°, *i.e.* even when this requires quite gross feed translations with larger scanning angles generally require more fundamental changes.

Although relatively unusual, it is possible to utilize a spherical main reflector [4] within the CATR system. Here, the feed is positioned at a distance from the vertex that is twice the radius of the spherical reflector with the other critical design parameters remaining unaffected. The respective surface profiles only differ appreciably at wider angles as subtended at the feed. For smaller angles, there is comparably little difference meaning that if the focal length is large compared to the reflector diameter, the folded optics produce a very viable CATR and are particularly attractive for sub-mm-wave applications [4]. Additionally, and by virtue of their geometry, the invariance of the CATR QZ to the scan angle about the symmetrical, *i.e.* offset makes them particularly attractive for scanning applications. Changing the orientation of the feed will correspondingly change the field illuminating the reflector and therefore the reflector edge diffraction, this effect can be mitigated providing the reflector is sufficiently large that changes in edge diffraction can by managed.

One effect that cannot be entirely corrected is the phase taper that is introduced in the QZ as a result of the spherical surface profiles where this difference is twice as significant in the offset axis as in the orthogonal axis. This difficulty can of course be entirely resolved if a parabolic profile were used in this axis. Thus, adopting a parabolic profile in the offset axis and a circular profile in the symmetrical axis produces the optimum CATR main reflector surface profile for scanning applications. The so called parabolic-toroid reflector [5] has been used in tracking applications, *e.g.* for ground station satellite tracking. However, the unique properties of this geometry have *not* previously been utilized within the folded optics of a CATR. The next section presents the results that illustrate the new CATR.

II. Results

Figure 1 presents the amplitude of the pseudo plane wave in the parabolic CATR (PCATR) QZ at $z = 5/3f$, where f denotes the focal length, as a false color checkerboard plot across a plane that is transverse to the longitudinal axis of the range. Figures 2 and 3 presents, respectively, equivalent plots for the spherical (SCATR) and parabolic toroid (PTCATRS). Figures 4, 5 and 6 present the phase of the copolar QZ for the PCATR, SCATR and PTCATR. From inspection of these figures the PCATR and PTCATRs provide very similar QZ performances. The amplitude pattern of the SCATR could be improved by repointing the elevation tilt of the feed, however the degraded phase performance, *cf.* Figure 5, is largely unavoidable for this f/D. Usefully, from inspection of Figures 7, 8 and 9 it is evident that the cross-polar QZ performance is largely independent of the profile of the respective main reflectors being examined.

The authors are pleased to acknowledge that this work was supported in part by Huawei Technologies GmbH.

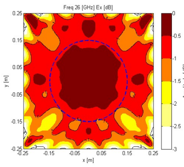

Fig. 1. PCATR Co-pol QZ amp

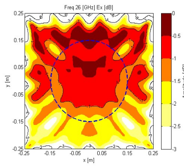

Fig. 2. SCATR Co-pol QZ amp

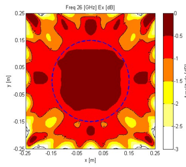

Fig. 3. PTCATR Co-pol QZ amp

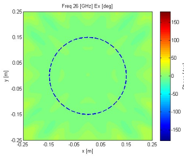

Fig. 4. PCATR Co-pol QZ phase

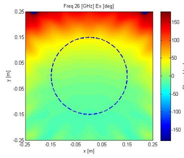

Fig. 5. SCATR Co-pol QZ phase

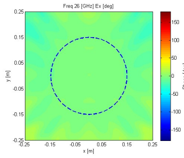

Fig. 6. PTCATR Co-pol QZ phase

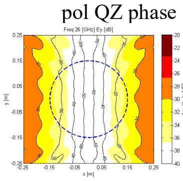

Fig. 7. PCATR X-pol QZ amp

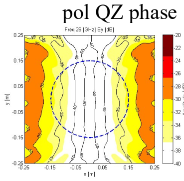

Fig. 8. SCATR X-pol QZ amp

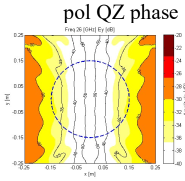

Fig. 9. PTCATR X-pol QZ amp

As there are larger differences between the copolar QZ performances, Figures 10, 11 and 12 respectively show plots of the amplitude at 0° blue, 45° green, 90° red and 135° cyan. The 0.3 m diameter target QZ size is shown in all plots as a blue dotted line. Here again, the PCATR and PTCATR yield very similar results with the SCATR exhibiting greater far variation, in the vertical axis. A similar observation can be made for the copolar phase plots which are presented in Figures the CATR QZ performances in the form of copolar and 13, 14 and 14.

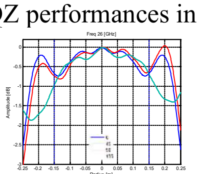

Fig. 10. PCATR Co-pol QZ amp cuts for

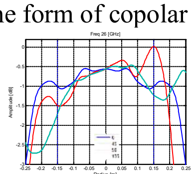

Fig. 11. Co-pol QZ amp cuts for SCATR

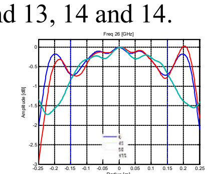

Fig. 12. Co-pol QZ amp cuts for PTCATR

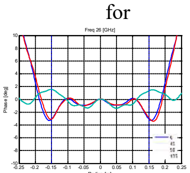

Fig. 13. Co-pol QZ pha cuts for PCATR

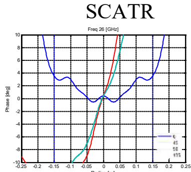

Fig. 14. Co-pol QZ pha cuts for SCATR

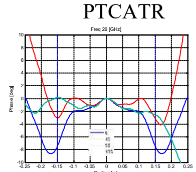

Fig. 15. Co-pol QZ pha cuts for PTCATR

A summary of the CATR QZ performance is presented in Table 1 below where the amplitude taper, amplitude ripple and phase ripple, which are the conventional performance criteria [4] are listed. These results illustrate that both the PCATR and PTCATR configurations satisfy the usual 1dB taper, ±0.5 dB amplitude ripple and ±5° phase ripple specifications [4].

TABLE I. SUMMARY OF CATR QZ PERFORMANCE @ 26 GHZ

0.3 m QZ Diameter	Parabolic	Spherical	Parabolic Toroid
Amp taper [dB]	0.91	1.13	0.87
Amp ripple [dB]	0.32	0.82	0.31
Phase ripple [deg]	3.27	72.8	7.3

To demonstrate the scanning concept, we have taken a f = 1.6 m focal length toroid with a 2.4 x 2.4 m reflector antenna and calculated the QZ max amplitude and phase ripple and amplitude taper in the fixed 30 cm diameter QZ located at $2f$ (3.2 m). Starting from the boresight case (Az = EL = 0°) moving the feed in elevation and z we can create scanned beams at ±15° in the fixed QZ. By moving the feed around the arc of the toroid focal length we can scan in azimuth and, adding an elevation scan achieves the example of a beam scanned in azimuth and elevation by 15°.

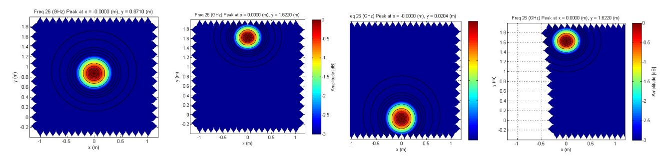

Fig. 16. 2.4m x 2.4m toroid reflector, scanned by feed movement, left to right: Az=El=0°; Az=0°, El=15°; Az=0°, El=-15°; Az=15°,El=15°

These 4 cases are illustrated in Figure 16 and the corresponding performance in terms of QZ performance is summarized in Table 2. These levels of QZ performance would produce high quality 5G characterization of the AUT over the scan range of Az = EL = ±15°. By increasing the size of the toroid reflector to 6.1 m wide and 2.4 m high, scan performance of Az =±60° and El=±15° can be achieved.

TABLE II. QZ AMPLITUDE AND PHASE PERFORMANCE FOR SCAN CASES SHOWN IN FIGURE 16

Scan	Max Amp Taper [dB]	Max Amp Ripple [dB]	Max Phase Ripple [deg]
Az = 0°, El =-15°	0.87	1.33	18.04
Az = 0°, El = 0°	0.61	0.01	0.16
Az = 0°, El =15°	1.09	0.60	13.32
Az = 15°, El = 15°	0.91	0.47	9.07

III. SUMMARY AND CONCLUSIONS

In this paper we have presented a novel CATR design that exhibits unique measurement attributes. The parabolic-toroid CATR offers wide scan angle operation across a very broad range of frequencies with QZ performance very nearly equal to that of a conventional parabolic main reflector CATR. The continuous reflector offers unlimited beam scanning in azimuth and elevation (with some limitations on how close two, or more, feeds can be placed without mechanical interference of the multi-axis robotic feed positioners). The chamber is significantly smaller and requires less than half the absorber that the best equivalent variable FF-MPAC can offer [6].

REFERENCES

[1] M. Gustafsson, T. Jämsä, M. Högberg, "OTA Methods for 5G BTS Testing – Survey of Potential Approaches", 32nd URSI GASS, Montreal, 19-26 August 2017.

[2] P. Kyosti, T.Jämsä, J.-P. Nuutinen, "Channel Modelling for Multiprobe Over-the-Air MIMO Testing", Hindawi, International Journal of Antennas and Propagation, Volume 2012, Article ID 615954.

[3] NR; Study on test methods, 3GPP TR 38.810: Release 16, Table 5.3-2, Page 29, March 2019.

[4] C.G. Parini, S.F. Gregson, J. McCormick, D. Janse van Rensburg "Theory and Practice of Modern Antenna Range Measurements", IET Press, 2014, ISBN 978-1-84919-560-7.

[5] W.L. Stutzman, G.A. Theil, "Antenna Theory and Design", 2nd Edition, John Wiley & Sons, 1998, Section 7.6.7, pp. 347 – 348.

[6] S.F. Gregson, C.G. Parini, "Examining and Optimising Far-Field Multi-Probe Anechoic Chambers for 5GNR OTA Testing of Massive MIMO Systems", EuCAP, Copenhagen, March 2020